

THE ABSORPTION OF NITRIC OXIDE IN THE  
NEAR INFRARED AND VISIBLE REGIONS  
IN LIQUID AND COMPRESSED GASEOUS STATES

CENTRE FOR NEWFOUNDLAND STUDIES

**TOTAL OF 10 PAGES ONLY  
MAY BE XEROXED**

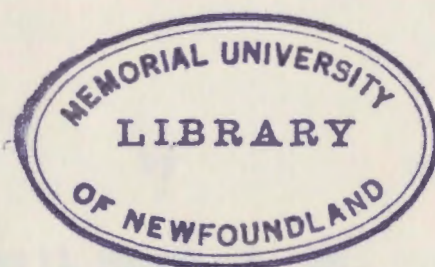
**(Without Author's Permission)**

CYRIL SNOOK

WIDE MITOCHONDRIA

DISCOIDIAL 23. 11. 1911

THE ASSOCIATION OF LIBRARIES IN THE  
NEW BRUNSWICK AND VICINITY  
IN NORTH AND WESTERN CANADA



Presented in partial fulfillment of the  
requirements for the degree of Master of Science  
Memorial University of Newfoundland

September, 1961





THE ABSORPTION OF NITRIC OXIDE IN THE  
NEAR INFRARED AND VISIBLE REGIONS  
IN LIQUID AND COMPRESSED GASEOUS STATES

by



Cyril Snook, B. Sc.

Submitted in partial fulfilment  
of the requirements for the degree of Master of Science  
Memorial University of Newfoundland

September, 1962

This thesis has been examined and approved by:

J. L. Hunt, B.A., M.A., Ph.D.

Assistant Professor

Memorial University of Newfoundland

E. J. Allin, M.A., Ph.D.

Associate Professor

University of Toronto

## TABLE OF CONTENTS

CHAPTER		Page
I	INTRODUCTION .....	1
II	THE SECOND OVERTONE ROTATION-VIBRATION BAND OF NITRIC OXIDE IN COMPRESSED GAS AND LIQUID .....	4
	Experimental Procedure	
	Results and Discussion	
III	THE ABSORPTION OF LIQUID NITRIC OXIDE IN THE VISIBLE AND NEAR INFRARED REGION .....	30
	Experimental Procedure	
	Results and Discussion	
APPENDIX		
	A STUDY OF 7620Å BAND OF OXYGEN IN LIQUID OXYGEN-ARGON MIXTURES .....	40
	Experimental Procedure	
	Results	
	SUMMARY .....	51
	BIBLIOGRAPHY .....	53
	ACKNOWLEDGMENT .....	55

## CHAPTER I

### INTRODUCTION

The absorption spectra of nitric oxide, one of the most interesting heteronuclear diatomic molecules which is chemically stable, has been extensively studied by various investigators; the study ranged from the ultraviolet to the microwave region (eg. 1-3). Because nitric oxide possesses an unpaired electron, a study of the electronic configuration in the molecule suggests that it has a permanent magnetic dipole moment and that its ground state is a  $^2\Pi$  state. The only other diatomic molecule which is known to possess a permanent magnetic dipole moment is oxygen, thus one may expect similar behaviour in both molecules with respect to magnetic effects.

Since the nitric oxide molecule possesses a permanent electric dipole moment all the rotation - vibration transitions are allowed transitions, unlike the homonuclear diatomic molecules. The fundamental rotation - vibration transition of nitric oxide in low pressure gas was first observed by Warburg and Leithauser in 1908 (28). Since then various investigators have studied the fundamental and overtone rotation - vibration bands in the low pressure gas using high resolution spectroscopic instruments (9,16,17). They found that the spectra showed the existence of Q branches in these infrared bands as was expected from the



theory of molecular spectra. The  $\Delta J = 0$  transition, which gives rise to the Q branch in infrared bands, is allowed in nitric oxide since nitric oxide possesses a non - zero resultant electronic orbital angular momentum about the internuclear axis.

A number of absorption band systems in the ultra-violet region, below approximately  $\lambda 2500 \text{ \AA}$ , have been observed by various investigators; these consist of the  $\gamma$ ,  $\beta$ ,  $\delta$ , and  $\epsilon$  bands of nitric oxide (20,1,21,8) as well as Tanaka's three Rydberg series of bands and others (26). The  $\gamma$ ,  $\beta$ ,  $\delta$ , and  $\epsilon$  ultraviolet bands are ascribed to various electronic transitions of the nitric oxide molecule.

In 1937 Vodar (27) studied the absorption spectrum of liquid nitric oxide in both the visible and ultraviolet regions. He observed that there were two extremely intense continua; one started at approximately  $\lambda 4000 \text{ \AA}$  extending toward the shorter wavelength side and the other at  $\lambda 5600 \text{ \AA}$  extending toward the longer wavelength side. Prior to this investigation Rice (19) predicted, from his theoretical treatment of its thermodynamical properties, that nitric oxide molecules are completely associated as  $(\text{NO})_2$  in the liquid. In 1946 Bernstein and Herzberg (2) also examined the absorption spectrum of liquid nitric oxide in the visible region. They also found these continua and suggested that the continua were due to the associated  $(\text{NO})_2$  molecules.

A similar suggestion for the existence of  $(O_2)_2$  complexes in liquid oxygen has also been made (14) and some of the anomalies in the spectrum of liquid oxygen have been explained in terms of the existence of  $(O_2)_2$  complexes (7). Since the magnetic property of nitric oxide is similar to that of oxygen it is not difficult to understand such a suggestion being made to explain the anomalies in the absorption spectrum of liquid nitric oxide. However, in the case of these continua of nitric oxide, especially for the continuum which occurs in the red region, it is very difficult to explain in terms of transitions which occur in  $(NO)_2$  complexes.

In the present investigation the second overtone rotation - vibration band of nitric oxide has been studied in compressed gas and in liquid. Since the absorption bands of oxygen in high density states exhibit marked dependence on the collision - induced transitions it is hoped to find the effects of intermolecular forces and association of  $(NO)_2$  molecules, if in existence, on the absorption band. The absorption spectrum of liquid nitric oxide in the near infrared and visible regions has also been studied in order to obtain better understanding of the behaviour of nitric oxide molecules in the liquid state.

A short report on a complimentary study of the O-O "Red Atmospheric" band of oxygen in liquid oxygen-argon mixtures is also given in Appendix.

CHAPTER II

THE SECOND OVERTONE ROTATION - VIBRATION BAND  
OF NITRIC OXIDE IN COMPRESSED GAS AND LIQUID

Experimental Procedure

The second overtone rotation - vibration absorption band of nitric oxide was studied in liquid and compressed gas at various pressures up to 150 atmospheres.

A) Gas Cells

A low pressure cell with an optical path length of 103 cm was used for pressures ranging from 22 p.s.i. to 160 p.s.i.; a high pressure cell with an optical path length of 12.5 cm was used for pressures ranging from 110 p.s.i. to 2500 p.s.i.

The long path - low pressure absorption cell, which was designed by M. J. Clouter (5), is shown in Figure 1. It consisted of an iron pipe, A, 100 cm in length and 1.5 cm inside diameter, and a glass tube, B, 100 cm in length and 1.3 cm inside diameter, which was inserted in A to serve as a light guide. On each end of the pipe, A, was screwed a steel end piece, C, accommodating a pressure sealed window, K. The windows, K, which were of 2 mm Pyrex glass plate with a diameter of 7/8 inch, were sealed with rubber cement to the inner surfaces of steel window plates, E, these plates were held in place by closing nuts, G. The apertures in the window

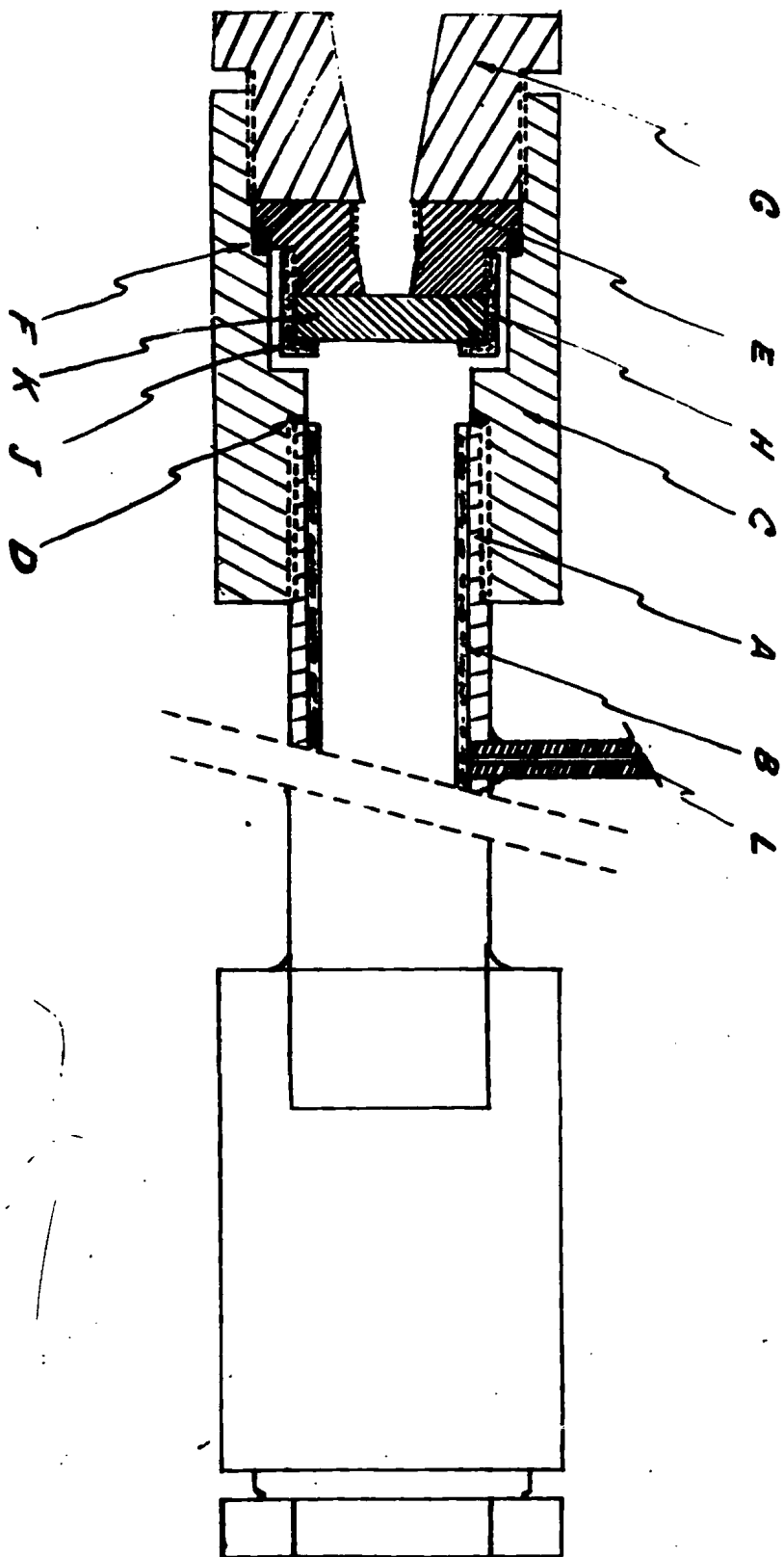


Figure 1. 100 cm gas absorption cell.

plates, E, were circular with  $1/4$  inch diameter; the inner surfaces of E, to which the windows were cemented, were polished optically flat. The windows, K, were secured by means of steel caps, H, screwed onto the window plates; Teflon washers, J, were used to prevent direct contact between the caps, H, and the windows, K. A  $1/16$  inch steel capillary tube, L, 24 inches in length, was brazed into the cell body to serve as a gas inlet; on the other end of the tube, L, an "Aminco" fitting was attached in order to make external connections.

In Figure 2 is shown the short path - high pressure absorption cell. The cell body, A, was constructed of stainless steel 3.5 inches in diameter with a  $.75$  inch bore. A stainless steel light guide, G, with a rectangular aperture, was inserted in the bore of the cell. Pyrex glass windows, W, 5 mm thick and with a diameter of  $7/8$  inch, were cemented onto the inner surfaces of stainless steel window plates, B, and secured by steel caps, C, with Teflon washers, D. The apertures in the window plates, B, were rectangular in shape with dimensions  $3/8$  inch by  $3/16$  inch; the inner surfaces of the plates, B, were optically flat in order to give a pressure seal when the windows, W, were cemented to the surfaces. The window plates, B, were sealed by heavy steel closing nuts, E, with Teflon washers, F, between the window plates, B, and the cell body, A. Portion B' of the window plate,  $3/8$  inch thick, was square in shape and fitted into a square recess in the body, A, thus preventing non - alignment of the rectangular opening in the





window plate and the rectangular opening in the light guide when the nut, E, was tightened. A 1/16 inch steel capillary tube, H, which served as a gas inlet, was connected to the cell by means of an "Aminco" fitting, I.

#### B) Liquid Cell and Cryostat

The cell and cryostat used in the study of absorption in liquid nitric oxide is shown in Figure 3. The cryostat consisted of two parts, A, B, which were sealed together by an O - ring, O. Part A was constructed from a brass cylinder, 23 cm long and 10 cm in diameter, which was soldered to an inner brass cylinder, 20 cm long and 8 cm in diameter. The inner cylinder served as a liquid air reservoir. A copper post, D, 4 cm long and 2 cm in diameter, was attached at the base of the inner cylinder by means of a copper ring, F, 1 cm thick and 4 cm in diameter. The copper post, D, supported the copper cell holder, E, which was 8 cm long and 2 cm in diameter. The heat conduction between the ends of the post, D, was controlled by means of a heater, H<sub>1</sub>, and a center bore, G; the center bore opened into the liquid air reservoir of the cryostat.

Part B consisted of a brass cylinder 6.5 cm long and 10 cm in diameter. The entrance and exit windows, W, were 2.54 cm in diameter and 2 mm thick. They were made of Pyrex glass plate and were cemented onto part B by means of sealing wax. The cryostat was evacuated by means of an outlet attached to B.

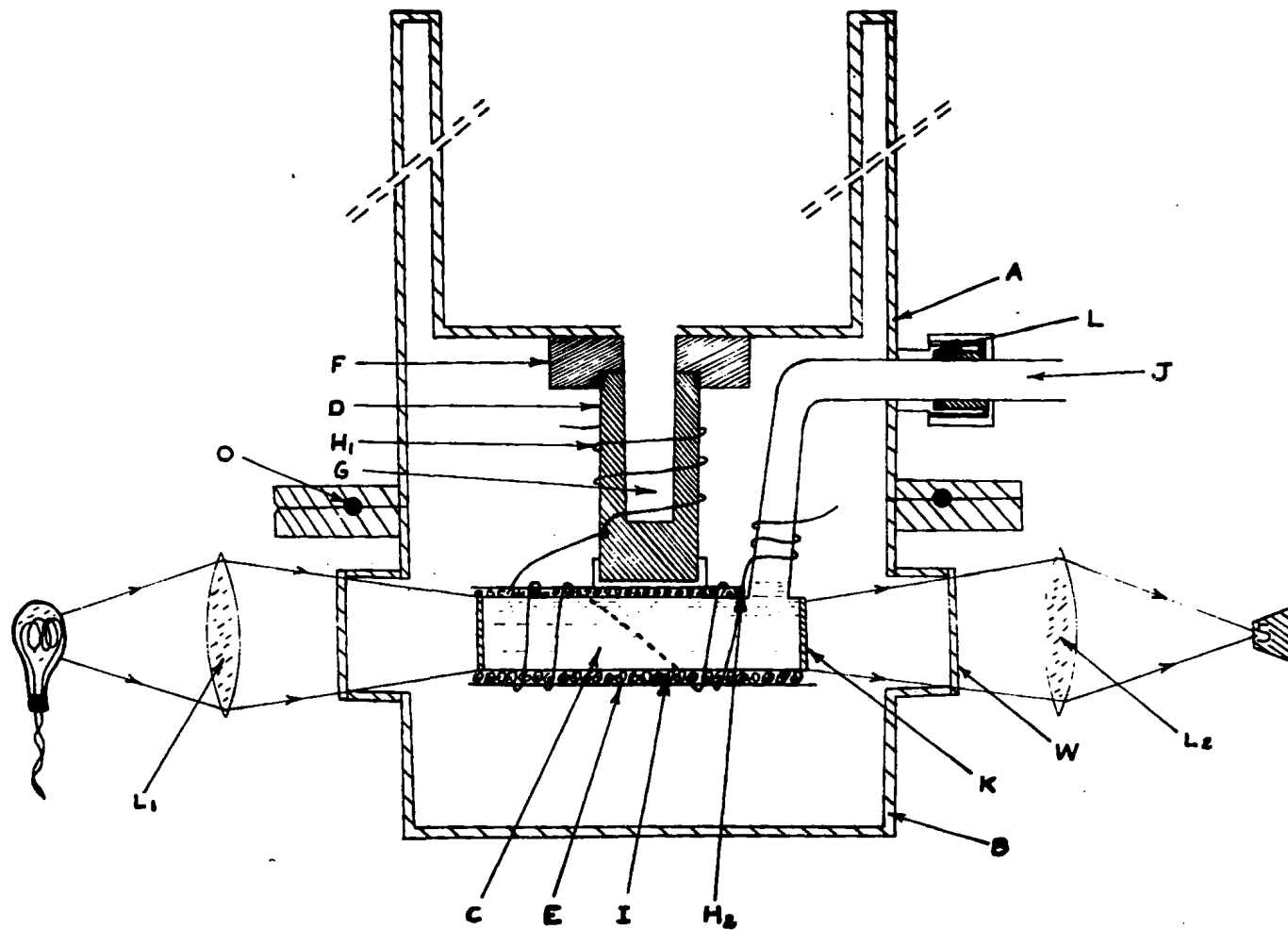


Figure 3. Low temperature cryostat and liquid cell used in the investigation of liquid NO.

An absorption cell, C, which was made of Pyrex glass, was placed inside the holder, E; the space between the cell and the holder, E, was filled with copper wool, I, in order to increase the efficiency of heat transfer between the cell and the holder. The windows of the cell, K, were of Pyrex glass, 1.5 cm in diameter and 1 mm thick and were fused into the body of the cell. A heater,  $H_2$ , which was independent of  $H_1$ , was mounted on the cell holder, E, and inlet tube, J, and served as a temperature control for the cell. Two cells were used with path lengths 7.7 cm and 1.1 cm. An outlet tube, J, was passed through the outer wall of the cryostat by means of an O - ring seal, L.

#### C) Purification Procedure for Nitric Oxide

Before nitric oxide gas, from a commercial cylinder, was introduced into the cell a careful purification step was necessary in order to eliminate the possible impurities of  $N_2O_3$ ,  $N_2O$ ,  $NO_2$ ,  $N_2$  and  $CO_2$  (13). It has been suggested by previous investigators that the removal of  $N_2O_3$  (m.p.  $-103^\circ C$ ) is more difficult than the removal of other impurities (27).

In Figure 4 the procedure for purification used in the present investigation is shown schematically. Nitric oxide gas from a commercial cylinder was allowed to solidify in the liquid air trap, A. When a sufficient amount of the gas had solidified the stopcock,  $S_1$ , was closed and the solidified nitric oxide was then opened to the vacuum pump for a period

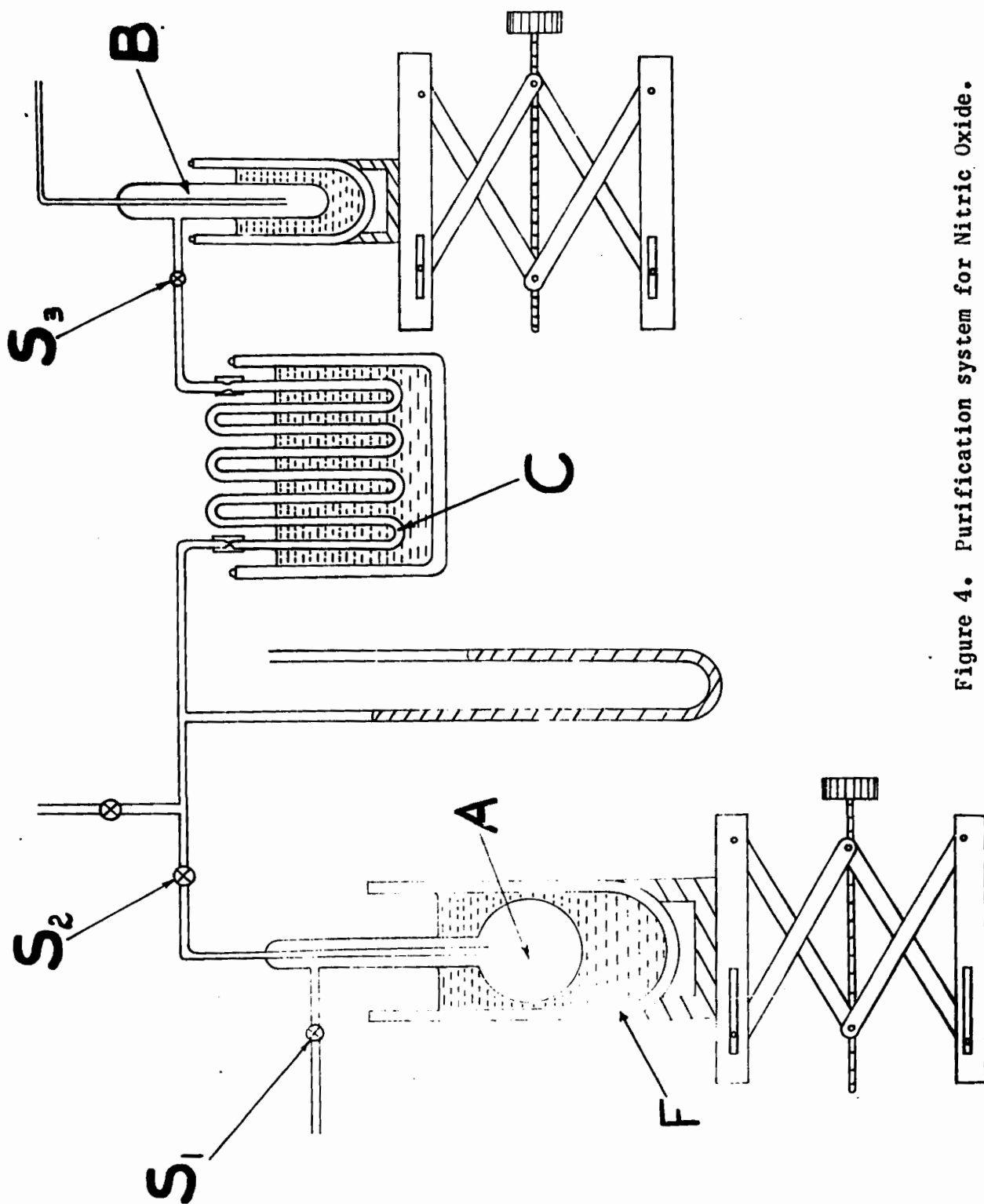


Figure 4. Purification system for Nitric Oxide.

of a few minutes to remove any nitrogen gas impurity. The dewar, F, which was mounted on a labjack, was then lowered and stopcock, S<sub>3</sub>, was adjusted to provide a slow flow of gas into another liquid air trap, B. The gas in passing from trap A to trap B, passed through the intermediate trap, C. The vapor pressure of the liquid nitric oxide in trap A was controlled by adjusting the liquid air level in the dewar, F. The rate of flow was so adjusted that approximately 2 cc of liquid nitric oxide was collected in the trap, B, per hour. Since the melting points of all known impurities are considerably higher than the melting point of nitric oxide (m.p.  $-163.6^{\circ}\text{C}$ ), the above procedure of slow flow served as a fractionation process. The trap, C, consisted of a series of four U tubes which were surrounded by solid or highly viscous ethyl alcohol at a temperature ranging from  $-110$  to  $-120^{\circ}\text{C}$ .

The color of the solid condensed in the trap, B, was found to be white with a slight tint of violet. This color was quite different from the bright blue color of  $\text{N}_2\text{O}_3$  which was observed in the trap C. The color of the purified liquid nitric oxide was pale blue similar to the color of liquid oxygen (13,27). The color of the liquid condensed in the trap, B, thus confirmed that the purification procedure was very effective. Following the above purification procedure approximately 1.5 times as much purified liquid was prepared in the trap B as was needed to fill the absorption cell.

## D) Experimental

### 1. Gaseous Nitric Oxide

Prior to its introduction into the cell the gas, purified as described in section C, was condensed in a steel thermal compressor. The thermal compressor consisted of a steel cylinder 2 inches in diameter and 8 inches in length with a 1/4 inch bore of length 7 inches. A 1/16 inch steel capillary tube, with an "Aminco" fitting at one end, was brazed into the bore of the thermal compressor to serve as a gas inlet. The condensation of the nitric oxide into the thermal compressor was accomplished by cooling the compressor with liquid air. The thermal compressor was connected to a pressure gauge and to the cell through a high pressure needle valve.

After a sufficient amount of nitric oxide was condensed into the thermal compressor the compressor was then isolated from the glass purification system by means of a check valve. The pressure gauge used, with a scale ranging from 0 - 2500 p.s.i., was calibrated with an Ashcroft test gauge, having a calibration ranging from 14.7 - 2500 p.s.i. The pressure in the cell was altered by opening the needle valve and allowing the temperature of the thermal compressor to rise, thus letting the required amount of gas into the cell. When a desired pressure of gas in the absorption cell was obtained the needle valve was closed, thus isolating the cell and the pressure gauge from the thermal compressor. The thermal compressor was then re-cooled to liquid air temperature. Nitric oxide gas was



thus obtained in the cell at pressures ranging from 0 - 2500 p.s.i.

The optical arrangement used with the cell is shown in Figure 5. Light from a source, R, is focused on the entrance window of the cell, C, by means of a spherical mirror,  $M_1$ , and a plane mirror,  $M_2$ . The light from the exit window is then focused on the slit of the spectrometer, S, by means of a plane mirror,  $M_3$ , and a spherical mirror,  $M_4$ . A light cone of size  $F/4$  was used to match the internal optics of the spectrometer.

In this investigation a Perkin-Elmer Model 12-C recording infrared spectrometer with a dense flint glass prism was used with a lead sulfide detector. The detector with its mount is shown in Figure 6. The mount was made of aluminum; a Kodak "Ektron" type N lead sulfide cell, C, was mounted on the flat portion, B', of the mount. The height of the cell was adjusted to the internal optics of the spectrometer. The lead sulfide detector was connected to the main amplifier, by means of a BNC connector, through a preamplifier which has been designed by H. Gush (11); the circuit diagram of the preamplifier with the component list is shown in Figure 7. The spectral slit width in the region of the band investigated ( $1.80\mu$ ) was  $3.5\text{ cm}^{-1}$ .

A 750 watt projection lamp, operating on 60 cycle power supplied through a Sorenson voltage regulator, served as a light source. A mercury arc emission spectrum was used for the wavelength calibration. The isothermal relation of gaseous

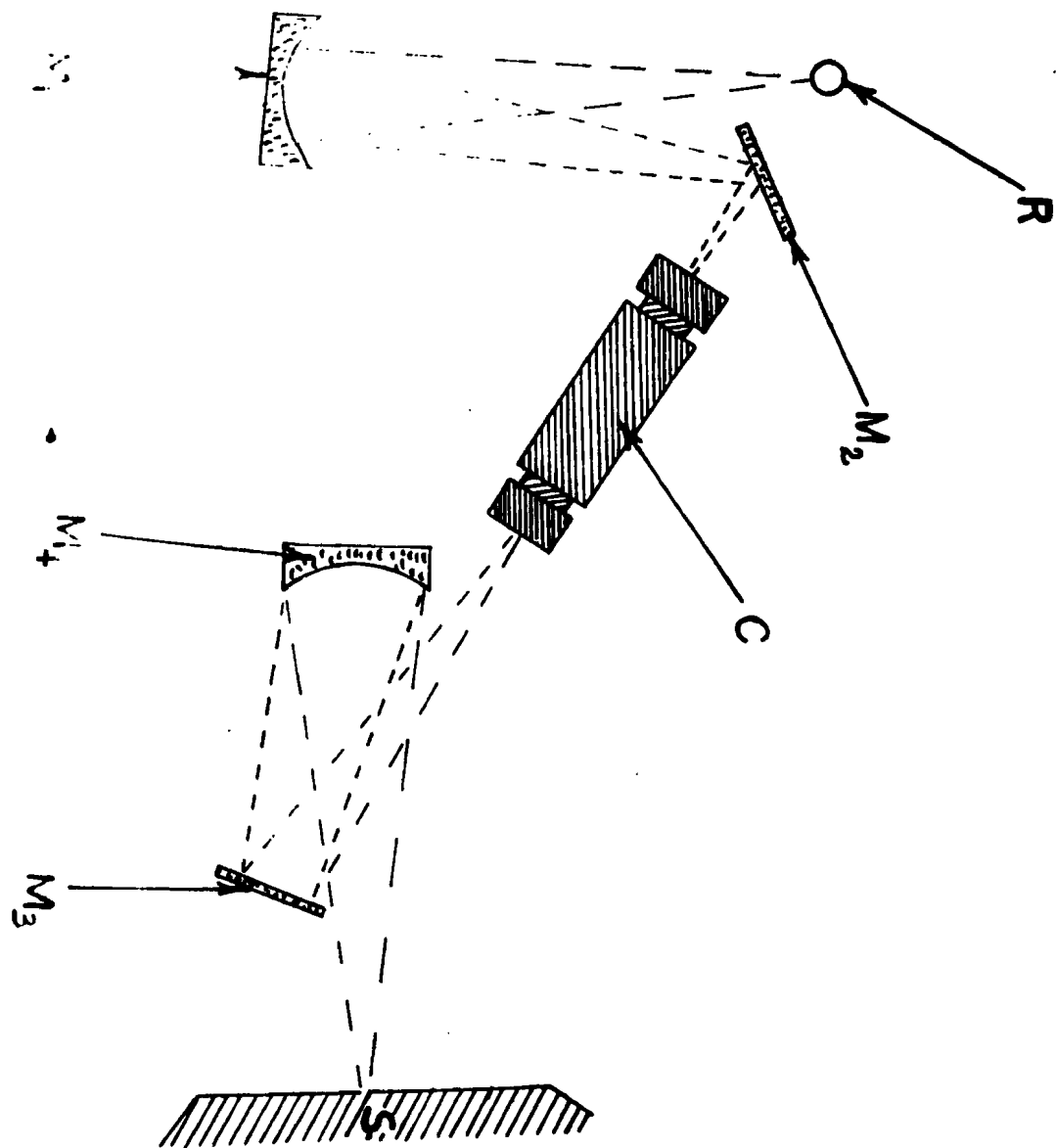


Figure 5. Optical arrangement for gas cells.

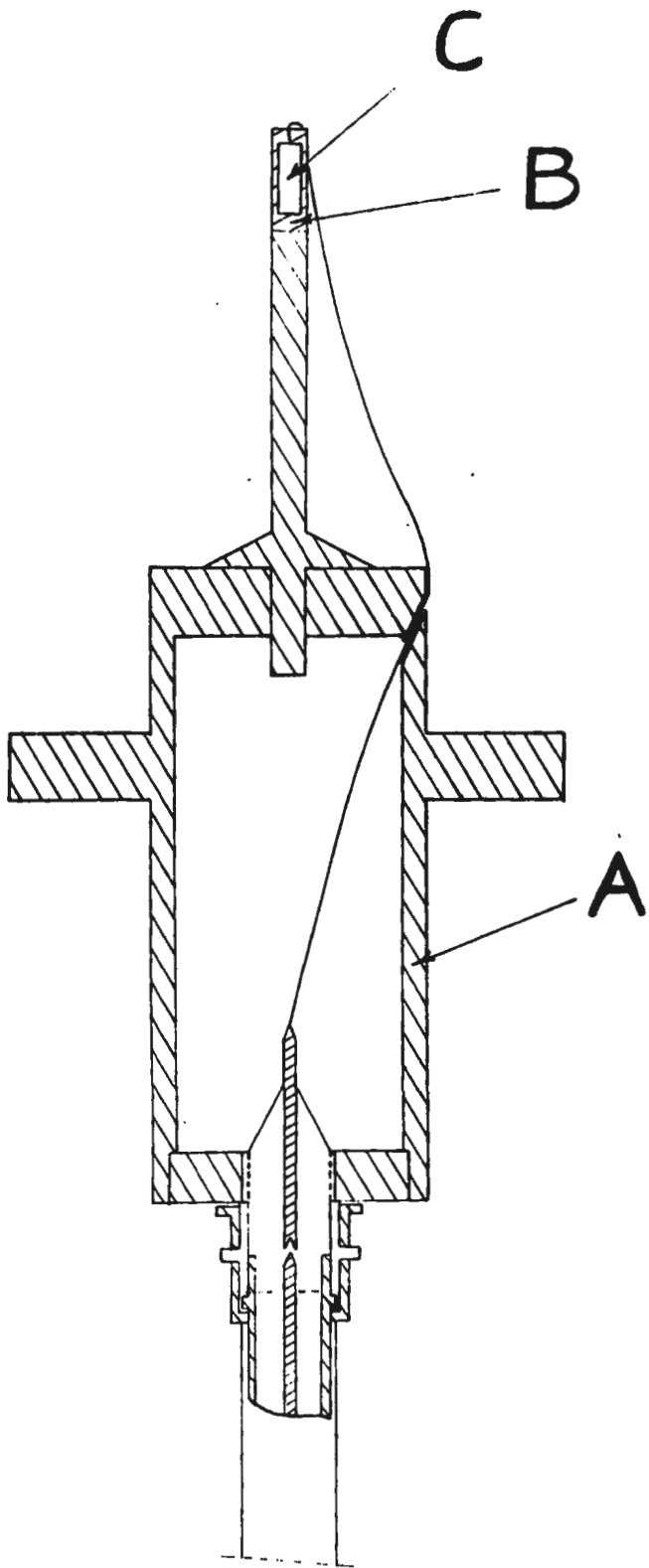
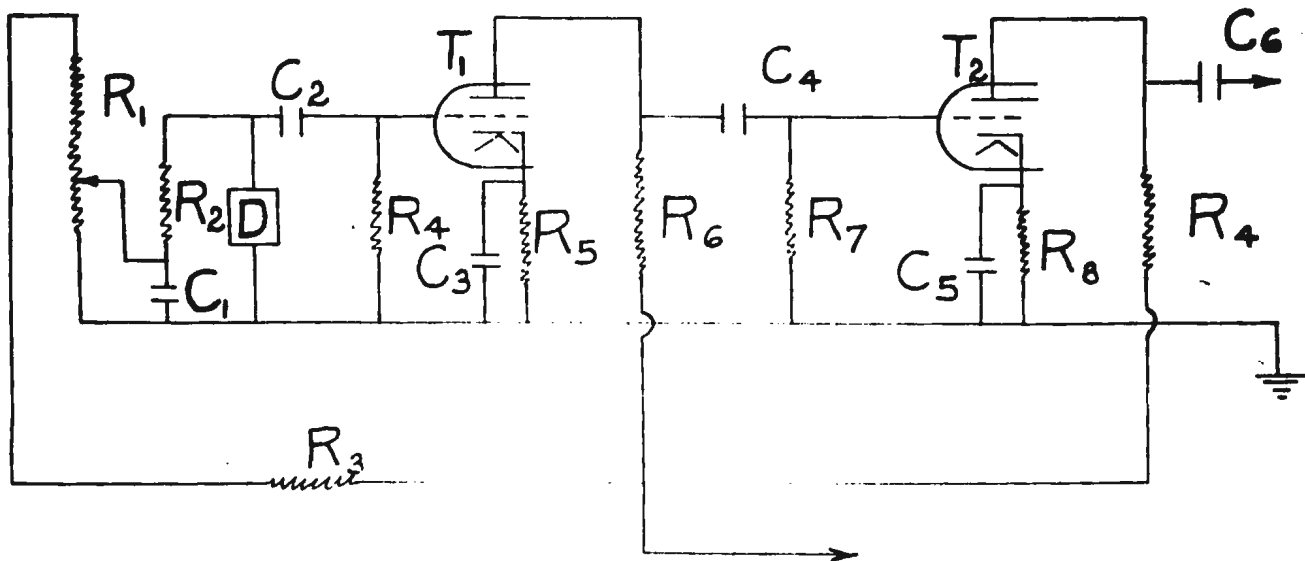


Figure 6. Lead sulfide detector and mount.



$R_1 - 250\text{ K}$

$R_2 - 6.8\text{ M}$

$R_3 - 500\text{ K}$

$R_4 - .22\text{ M}$

$R_5 - 3000\ \Omega$

$R_6 - .1\text{ M}$

$R_7 - .22\text{ M}$

$R_8 - 3000\ \Omega$

$R_9 - .1\text{ M}$

$C_1 - 70\text{ PF}$

$C_2 - .15\ \mu\text{F}$

$C_3 - 10\ \mu\text{F}$

$C_4 - .15\ \mu\text{F}$

$C_5 - 10\ \mu\text{F}$

$C_6 - .15\ \mu\text{F}$

$V - +90$

$T_1 - \frac{1}{2}12\text{AY7}$

$T_2 - \frac{1}{2}12\text{AY7}$

D - PbS DETECTOR

Figure 7. Circuit diagram of preamplifier.

nitric oxide for the pressure range 0 - 2500 p.s.i. was obtained, for a temperature of 298°K, by interpolating from data obtained in a previous investigation (10). The densities, in amagat units, were computed for the pressure range 0 - 2500 p.s.i. from the isothermal relation of nitric oxide at 298°K. The amagat unit of density is defined as the ratio of the density at a given pressure and temperature to the density at NTP. An absorption contour was produced by plotting the absorption coefficient,  $\alpha$ , which is defined as  $\log_e I_0/I$ , against the frequency in  $\text{cm}^{-1}$ ; here  $I$  is the intensity of light from a source after the light has passed through an absorbing material and  $I_0$  is the background intensity of the light measured at the same frequency but without the absorbing material in the path. The integrated absorption coefficient,  $\int \alpha d\nu$ , in  $\text{cm}^{-1}$  is then obtained by computing the area under the absorption contour.

## 2) Liquid Nitric Oxide

Before the purified nitric oxide gas was introduced into the absorption cell, contained in the cryostat, both the cryostat and cell were evacuated. The liquid air reservoir in the cryostat was then filled in order to precool the absorption cell.

The purified nitric oxide was condensed in the trap, B, of the purification system (Figure 4) and transferred into the absorption cell. The transfer was accomplished by controlling the temperature of the purified nitric oxide, and consequently its vapor pressure, by means of the liquid air dewar containing

the trap, B, (Figure 4). This procedure served as a fractionation process and was the last step in the purification of the nitric oxide. The 1.1 cm absorption cell was filled in about 45 minutes and the 7.7 cm absorption cell was filled in about 90 minutes. The temperature of the absorption cells was controlled by means of the heaters  $H_1$  and  $H_2$  (Figure 3). Measurements of the temperature were made by means of an iron - constantan thermocouple, fixed into the cryostat by means of "Fusites" (23). The cells were kept at a temperature of  $-160 \pm 2$  °C. The color of the liquid inside the short cell was pale blue, the same as was seen in the trap, B, (Figure 4). The color of the liquid seen inside the long cell was a deeper blue than that seen inside the short cell, due, probably, to the greater path length.

The optical arrangement and equipment described in section D - 1 on gaseous nitric oxide was also used in this investigation. The spectral slit width used was  $3.5 \text{ cm}^{-1}$ . A 750 watt projection lamp, operated through a Sorenson voltage regulator, was used as a light source. A mercury arc emission spectrum was used for the wavelength calibration.



## Results and Discussion.

The second overtone rotation - vibration absorption band of nitric oxide was studied in liquid and gaseous nitric oxide. In the study of gaseous nitric oxide two cells were used with path lengths of 10 cm and 103 cm at pressures ranging from 20 p.s.i. to 2500 p.s.i. In the study of liquid nitric oxide path lengths of 1.1 cm and 7.7 cm were used; the temperature of the liquid was  $-160 \pm 2$  °C.

In Figure 8 a comparison is made of the absorption profiles of gaseous nitric oxide at three pressures, 150 p.s.i., 1060 p.s.i. and 1750 p.s.i. The intensity scale is adjusted for each curve to give the same area under each of the three contours. It can be seen that there is no significant change in the shapes of the contours within experimental error.

In Figure 9 is shown an observed contour of the second overtone rotation - vibration band with the theoretical intensities for the rotational lines, at 296 °K, which were calculated from the molecular data of nitric oxide given in the literature (12), the band origin is indicated by  $\nu_0$ . Because of its electronic configuration nitric oxide has a doublet ground state  $^2\Pi_{1/2,3/2}$ ; the two states being separated by  $121\text{ cm}^{-1}$ . All the rotational lines in this band are therefore doublets; the solid and broken lines in the theoretical fine

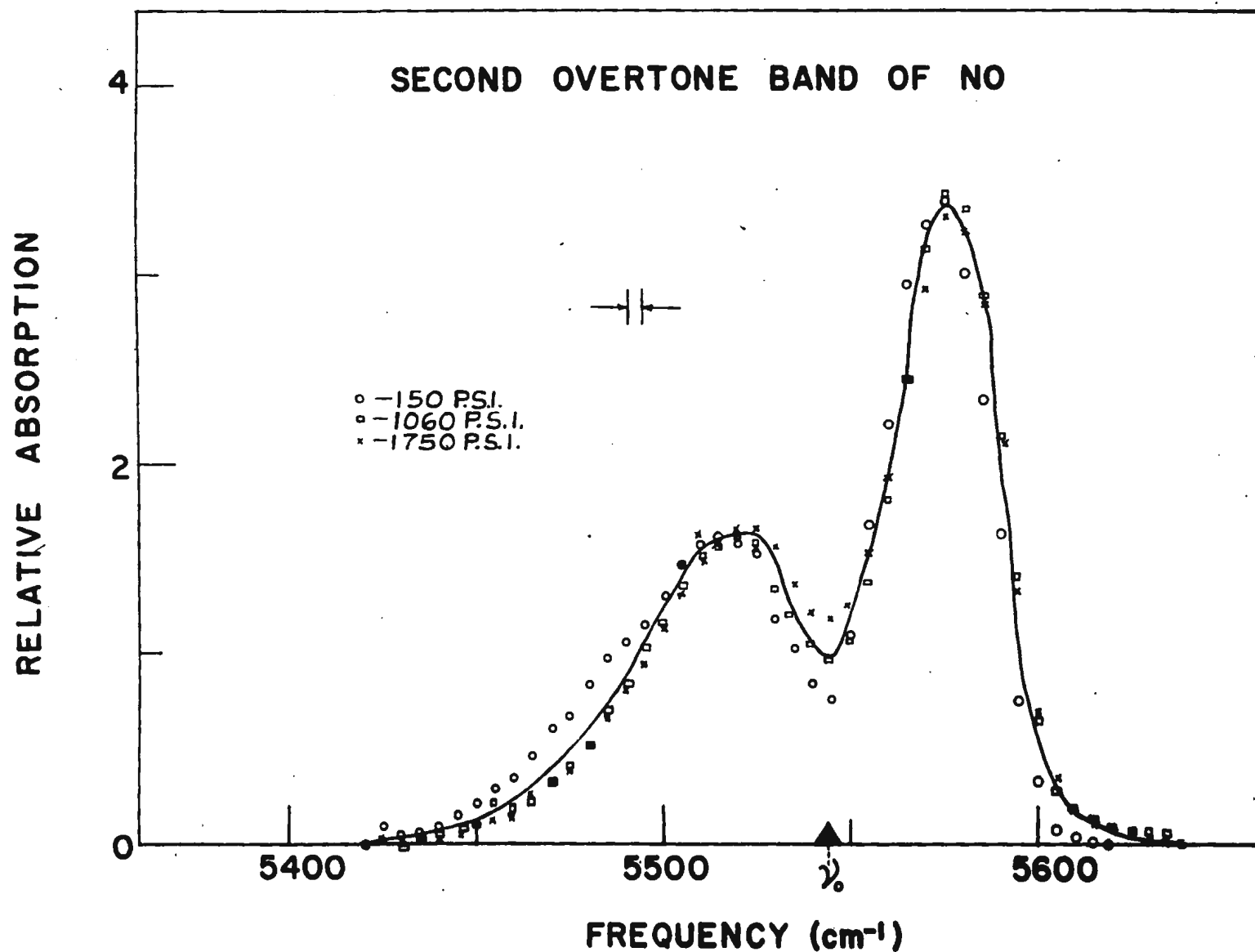


Figure 8. Normalized absorption contours of the second overtone rotation - vibration absorption band of nitric oxide.

# SECOND OVERTONE ROTATION-VIBRATION BAND

RELATIVE ABSORPTION

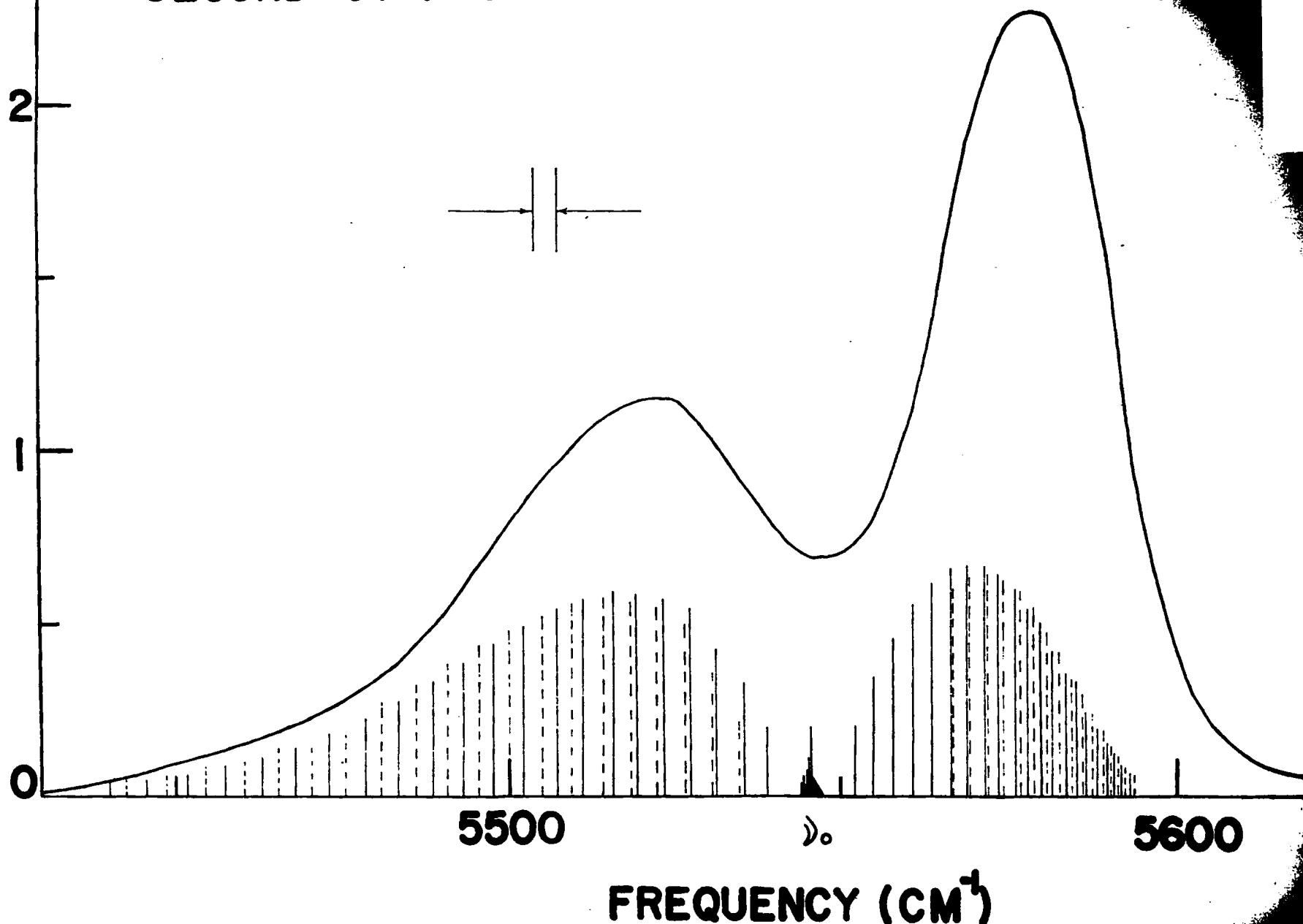


Figure 9. Comparison of the observed contour and theoretical intensity distribution for the second overtone rotation-vibration absorption band of nitric oxide.

structure indicate transitions in  $^2\Pi_{1/2}$  and  $^2\Pi_{3/2}$  states respectively. The length of each line in the calculated fine structure is drawn to be proportional to the transition probability of the corresponding rotational transitions. Since the ground state of the nitric oxide molecule is not a  $\Sigma$  state, rotation - vibration bands possess a Q branch as well as P and R branches. However, the intensity of the Q branch is very weak compared with the intensities of the other branches thus giving the observed absorption contour the appearance of a Bjerrum double band with a missing Q branch. This has been verified by various investigators who have studied the fundamental and first and second overtone bands of nitric oxide at low pressure (9, 16, 17).

For a Bjerrum double band, the separation of the peaks of the P and R branches are dependent on the temperature; with increasing temperature the intensity maxima of the two branches move outward. If in an unresolved band the maxima of the P and R branches can still be recognized and their separation measured a value for the rotational constant, B, may be obtained if the temperature is known. The separation of the two maxima is given by

$$\Delta\nu_{PR}^{\max} = \sqrt{\frac{8 B k T}{hc}}$$

where B is the rotational constant of a molecule  
 k is Boltzmann's constant  
 T is the temperature in  $^{\circ}\text{K}$   
 h is Planck's constant  
 and c is the velocity of light. (12)

From the contour in Figure 9, the separation of the P and R branches was found to be  $55\text{ cm}^{-1}$  at a temperature of  $298^{\circ}\text{K}$ , thus giving the rotational constant, B, to be  $1.8\text{ cm}^{-1}$ . The rotational constant, B, calculated for the second vibrational state is  $1.66\text{ cm}^{-1}$  (12). The slight deviation of the observed value from the theoretical value is probably due to the shift of the R branch toward shorter wavelengths because of the denser distribution of the rotational lines for higher J values in the computed R branch than in the P branch. This is partially compensated for by the shift of the R branch towards longer wavelengths by the presence of the Q branch. The total intensities of the P and R branches are also compared. The sum of the intensity of the theoretical rotational lines in the P branch is compared with the sum of those in the R branch. The ratio between the two sums is found to be 1:1.16 for P:R. Two areas under the absorption contour above and below the band origin  $\nu_0$  are measured separately in order to make a comparison. The ratio between two areas is found to be 1:1.17 for P:R. This seems to indicate that the intensity of the Q branch affects very little the general appearance of the band. It is important to note that there was no indication of the presence of any other branches which might be expected as a result of pressure induced absorption.

It was impossible to observe the second overtone

rotation-vibration band of nitric oxide in liquid due to the presence of a very strong continuum which was observed in this region ( $1.80\mu$ ).

The nature of this continuum will be discussed in the next Chapter.

In Table I are given the observed integrated absorption coefficients,  $\int \alpha d\nu$ , of gaseous nitric oxide at various densities. The integrated absorption coefficient is plotted against the density of the gas,  $\rho_{\text{NO}}$ , in Figure 10. From the plot it can be seen that the curve exhibits a fairly close linear relationship but it also indicates a second order deviation. It has been found that the absorption of an actual gas at high pressures does not in general obey Beer's law but follows the relationship,

$$\int \alpha d\nu = \alpha_0 \rho + \alpha_1 \rho^2 + \alpha_2 \rho^3 + \dots$$

where  $\alpha_0, \alpha_1$ , and  $\alpha_2$  are constants and  $\rho$  is the density of the pure gas. The first term indicates absorption which is due to the intrinsic transition of the molecule; the second and the third term are due to the binary and ternary collision induced transitions respectively. Therefore, in order to determine the constants  $\alpha_0, \alpha_1$ , etc. the specific integrated absorption coefficient  $\int \alpha d\nu / \rho_{\text{NO}}$  is plotted against  $\rho_{\text{NO}}$  in Figure 11. From the plot it can be seen that a straight line is a good approximation in representing the relationship. The intercept of the straight line with



Table I

ABSORPTION COEFFICIENT OF THE  
SECOND OVERTONE BAND OF NITRIC OXIDE  
AT VARIOUS GAS DENSITIES

$\rho_{NO}$ (Amagat Units)	$\int \alpha d\nu$ (cm <sup>-1</sup> /cm)	$\rho_{NO}$ (Amagat Units)	$\int \alpha d\nu$ (cm <sup>-1</sup> /cm)
2.30	.1031	9.92	.453
2.33	.0821	10.45	.447
2.94	.108	10.7	.385
3.43	.158	11.0	.508
3.59	.137	15.0	.642
4.14	.159	20.2	.853
4.21	.165	25.4	1.02
4.81	.197	33.9	1.41
5.30	.248	40.8	1.64
5.40	.232	43.8	1.88
5.46	.231	44.9	1.93
6.02	.244	48.7	2.11
6.11	.265	57.8	2.56
6.62	.289	61.1	2.68
6.73	.292	64.8	2.71
6.80	.202	70.2	3.15
7.25	.328	84.8	3.35
7.37	.321	97.4	3.88
7.47	.360	99.0	4.74
7.91	.300	115.8	5.23
8.52	.391	118.0	4.92
8.65	.403	130.0	6.11
9.15	.415	144.7	7.17
9.29	.424	166.6	7.82
9.74	.452		

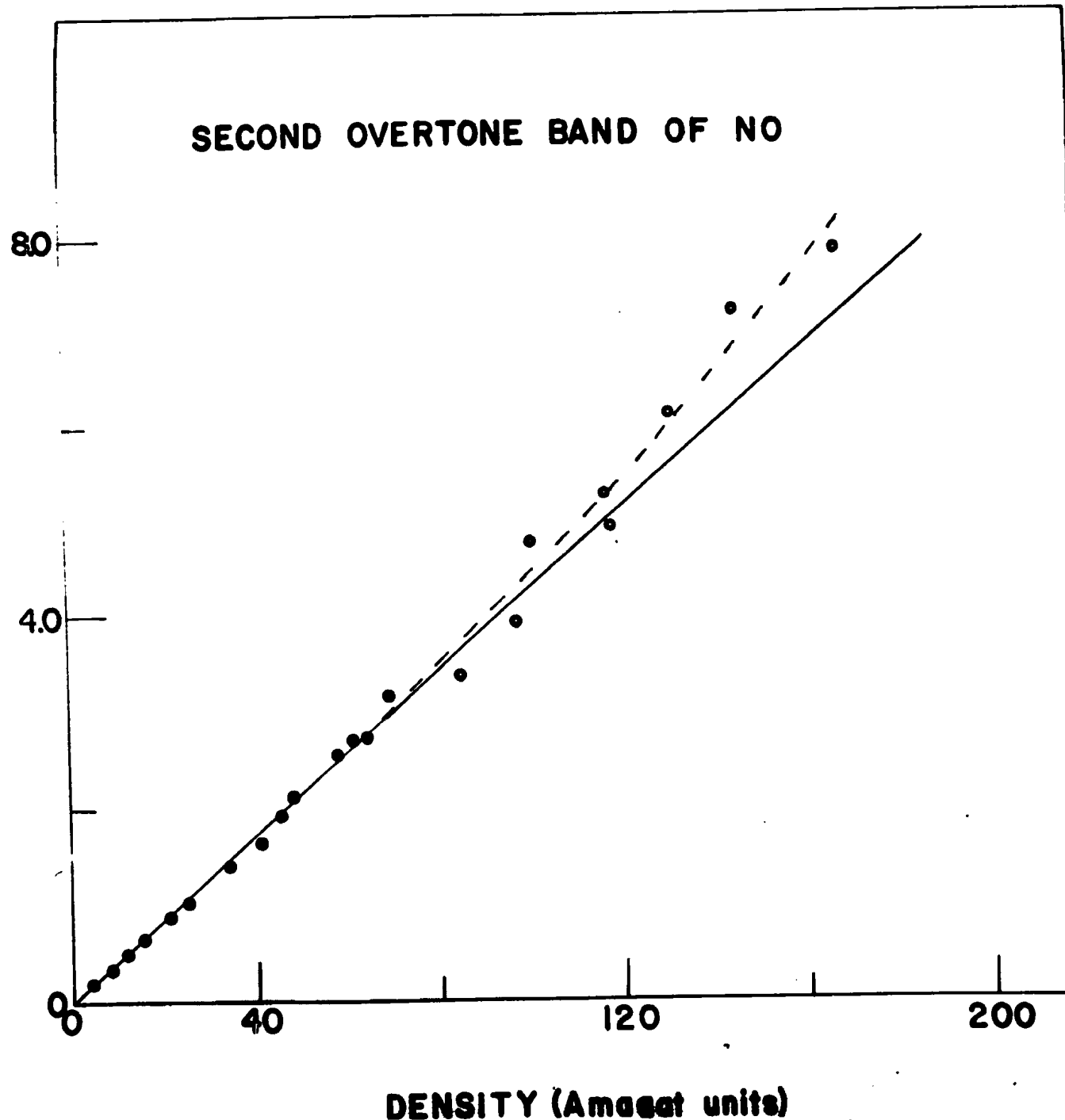
$\int \alpha p \, d\lambda \text{ (cm}^{-1}\text{/cm)}$ 


Figure 10. A plot of the integrated absorption coefficient of the second overtone rotation - vibration absorption band of nitric oxide against gas density.

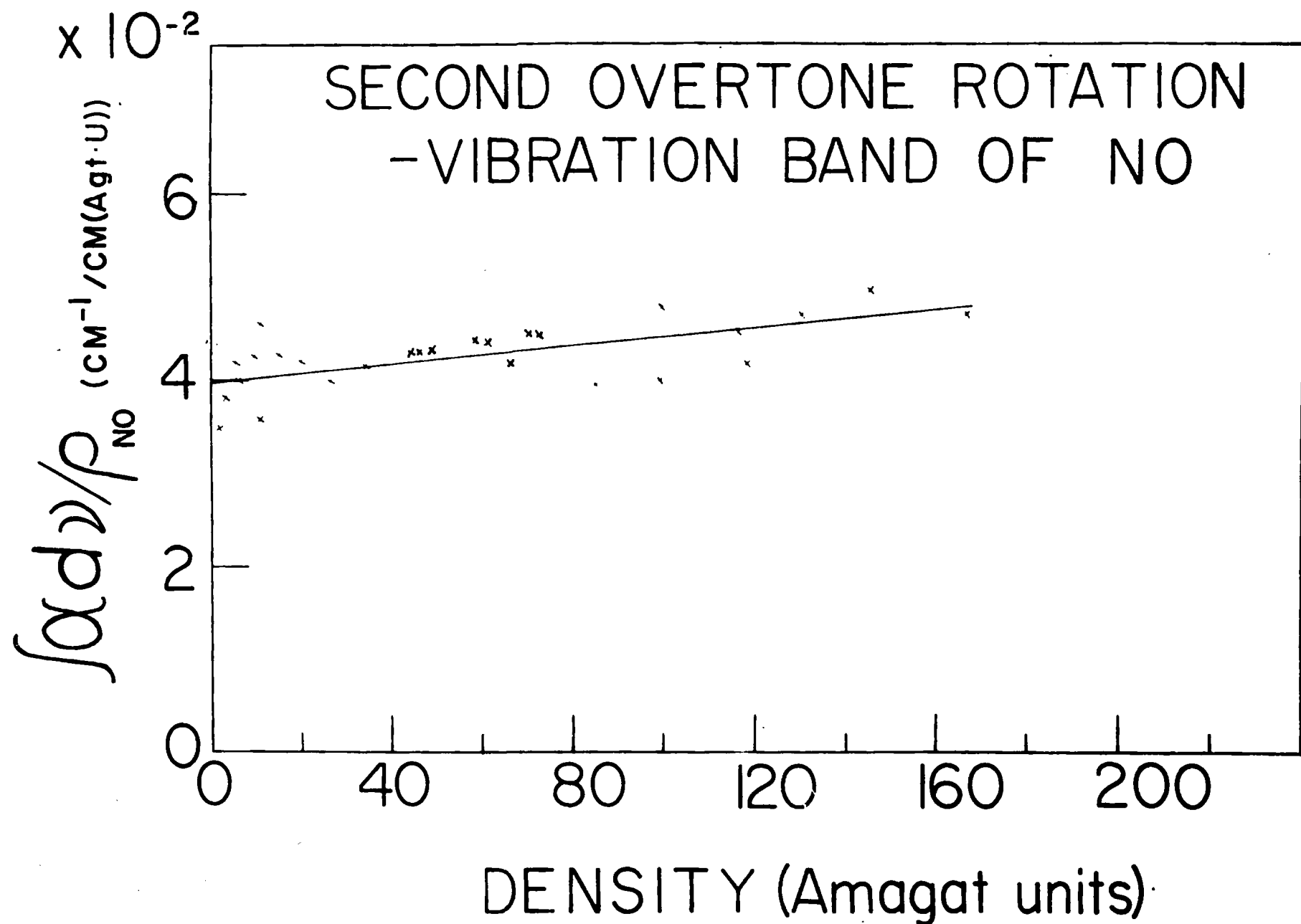


Figure 11. A plot of the specific integrated absorption coefficient of the second overtone rotation-vibration absorption band of NO against density

the ordinate gives  $\alpha_0 = 4.0 \times 10^{-2} \text{ cm}^{-1}/\text{cm}/ \text{Amagat unit}$  and from the slope one can determine that  $\alpha_1 = 4.9 \times 10^{-5} \text{ cm}^{-1}/\text{cm}/(\text{Amagat unit})^2$ . Therefore, one can derive the intensity relation at the present range of densities as follows:

$$\int \alpha d\nu = 4.0 \times 10^{-2} \rho_{\text{NO}} + 4.9 \times 10^{-5} \rho_{\text{NO}}^2$$

where  $\int \alpha d\nu$  is expressed in  $\text{cm}^{-1}/\text{cm}$  and  $\rho_{\text{NO}}$  is expressed in Amagat units.

Higher order terms which might exist in the relationship were not observable in the present pressure range. From the intensity expression the ratio between the intensities due to intrinsic transitions and pressure induced absorption may be computed at any given pressures. According to calculation, even at the highest pressure which was obtained in this investigation, 2400 psi, approximately 80% of the total absorption is still due to intrinsic transitions. It is therefore concluded that the study of pressure induced effects on this absorption band cannot be carried out until the density of the gas reaches at least 800 Amagat units. At this density the intensity due to intrinsic transitions becomes approximately 50% of the total absorption. It is therefore very regrettable that the absorption band in liquid nitric oxide was unable to be observed.

### CHAPTER III

## THE ABSORPTION OF LIQUID NITRIC OXIDE IN THE VISIBLE AND NEAR INFRARED REGION

### Experimental Procedure

The absorption spectrum of liquid nitric oxide in the visible and near infrared regions was studied using the liquid cells and cryostat described in the previous chapter.

In this study the visible and near infrared regions were studied using a Hilger constant deviation glass spectrograph. In Table II, the spectral slit widths, types of plates and comparison spectra which were used in this investigation are shown.

Table II

#### SPECTROGRAPHIC DATA

Optical Region	Type of Plate	Spectral Slit Width	Comparison Spectrum
3,500 - 6,600 $\text{\AA}$	Kodak Super Panchromatic	7.0 $\text{cm}^{-1}$ (4000 $\text{\AA}$ )	Iron Arc
6,600 - 9,000 $\text{\AA}$	Kodak 1-N	7.1 $\text{cm}^{-1}$ (7000 $\text{\AA}$ )	Neon discharge
9,000 - 12,000 $\text{\AA}$	Kodak 1-Z (2)	9.1 $\text{cm}^{-1}$ (9000 $\text{\AA}$ )	Mercury Arc and Neon discharge

The Kodak 1-Z (2) plates were hyper-sensitized with a 1.2% ammonium hydroxide solution immediately before they were used.

The optical arrangement used with the spectrograph is shown in Figure 3. Light from a source, R, is focused on the entrance window, W, of the cell by means of lens L, the light from the exit window is then focused by means of lens, L<sub>2</sub>, onto the slit of the spectrometer, S.

A 750 watt projection lamp operating on 60 cycle power supplied through a Sorenson voltage regulator served as a light source.

The absorption contours obtained on the photographic plates were reduced using a Hilger recording microphotometer. The intensities were calibrated by means of a Hilger stepped sector.

## Results and Discussion

It was found in the study of liquid nitric oxide that there appeared to be complete absorption in the region where the second overtone rotation-vibration band would occur. In preliminary investigations this absorption was found to extend throughout the region between  $\lambda 1.2\mu$  and  $\lambda 1.80\mu$ , thus obscuring the observation of the second overtone rotation-vibration band. The investigation was therefore extended into the visible and near infrared regions in order to study the behaviour of the continuum.

In Figure 12 is shown the absorption profile of the red cutoff position of the continuum obtained by absorption cell with a path length of 1.1 cm. The ordinate in this plot represents Percent Absorption which has been estimated in comparison with the background spectrum. It can be seen in Figure 12, that the absorption starts at  $\lambda 8,600\text{\AA}$  and complete absorption begins at  $\lambda 9,300\text{\AA}$  and extends towards longer wavelengths. The continuum extends at least up to  $\lambda 1.2\mu$ , this has been verified using the infrared sensitive photographic plates. Therefore, the continuum which starts at  $\lambda 8,600\text{\AA}$  is found to extend to  $\lambda 1.80\mu$ . The behaviour of the continuum beyond  $\lambda 1.80\mu$  has not been studied since the glass optics were used in the present investigation and thus preventing observation

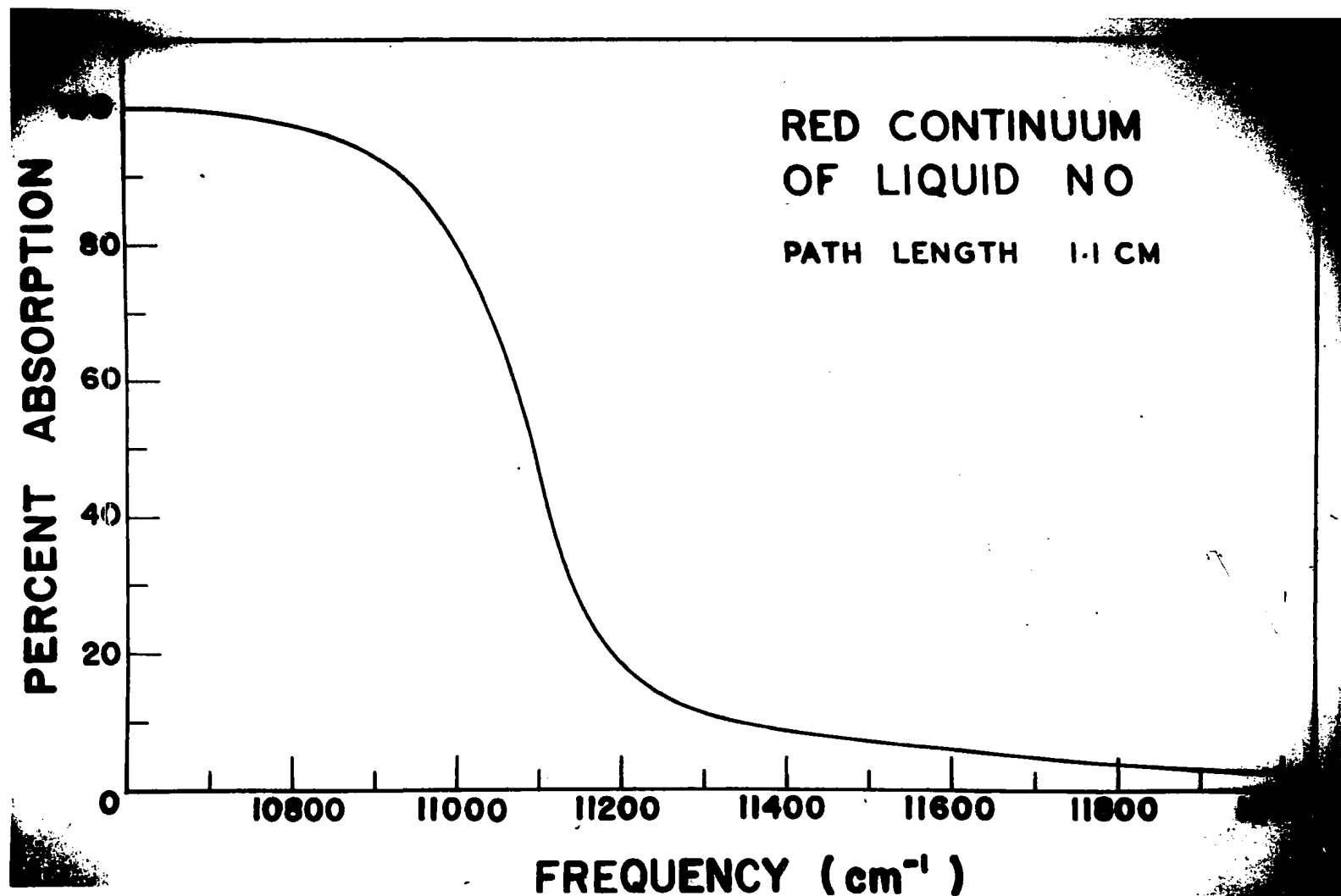


Figure 12. The cutoff of the red continuum in liquid Nitric Oxide.



of the spectrum at the wavelength beyond  $\lambda 1.8\mu$ . In the visible region another continuum, which starts at  $\lambda 4140 \text{ \AA}$  was found; the absorption profile of the cutoff of this continuum is shown in Figure 13. This violet continuum starts at  $\lambda 4140 \text{ \AA}$  and at  $\lambda 4070 \text{ \AA}$  there seemed to be complete absorption extending towards the shorter wavelength region. The above violet and red continua were also studied with the absorption cell of path length 7.7 cm. With this long path length cell it was found that the exposure time in photographing the spectrum was 10 minutes, as compared with an exposure time of 2 seconds for the background spectrum. This seemed to indicate overall absorption throughout the visible and near infrared regions, thus preventing the accurate reduction of the absorption profiles. With the spectrogram obtained using the long exposure time (10 minutes), it was found that there was a significant increase in absorption, in the red, starting at approximately  $\lambda 6600 \text{ \AA}$  and extending toward the infrared, and in the violet starting at approximately  $\lambda 4200 \text{ \AA}$  and extending toward the ultraviolet.

Vodar observed similar continua in liquid nitric oxide in the visible region using an absorption path length of 2 cm (27), and his results were later interpreted as being due to the presence of associated  $(\text{NO})_2$  molecules (2).

Bernstein and Herzberg have also studied the continua using a path length of 3 cm. According to their results the violet continuum started at  $\lambda 4000 \text{ \AA}$  and the red continuum started

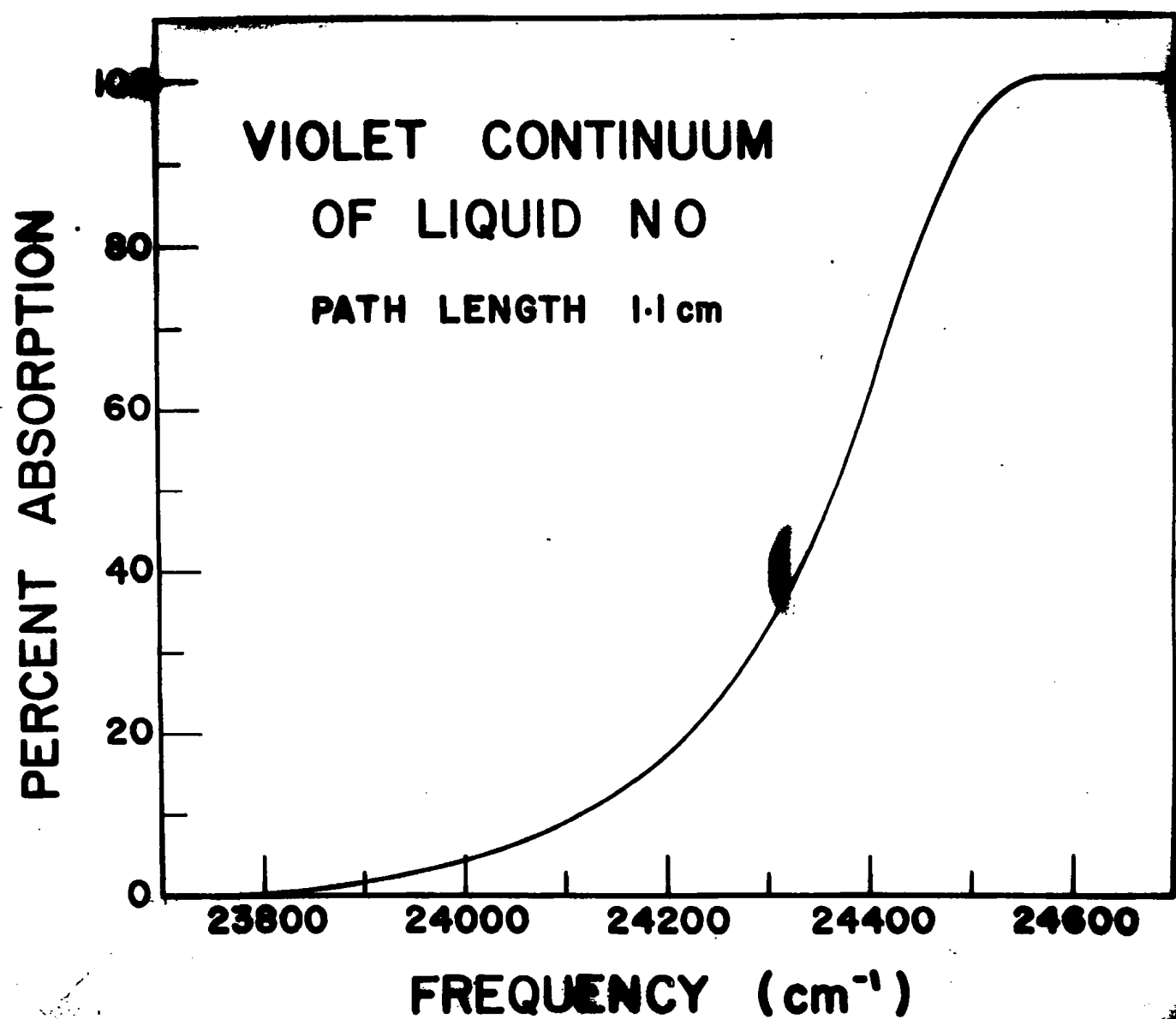


Figure 13. The cutoff of the violet continuum in liquid Nitric Oxide.

at  $\lambda 5,600\text{\AA}$  (2). Their investigations covered only the visible and the ultraviolet regions. Although the present observations were in general agreement with the results obtained by the above investigators, it appears that the cutoff wavelengths of the red continuum in the present investigation and in their investigations do not agree as well as those of the violet continuum. For nitric oxide gas at pressures up to 2,500 p.s.i. Stevenson (25) has observed the absorption spectrum of nitric oxide in the visible and near infrared regions using a path length of 10 cm. He found that the violet continuum starts to appear at pressures as low as 300 p.s.i. The cutoff wavelength of the continuum changes with pressure; being  $\lambda 3,830\text{\AA}$  at a pressure of 300 p.s.i. and reaching  $\lambda 4,100\text{\AA}$  at 2,500 p.s.i. It is also interesting to note that the cutoff wavelength of the violet continuum for the gas at 2,500 p.s.i. agrees very well with that of the liquid. The red continuum was not observed in the gas by Stevenson. In the course of the investigation described in the previous chapter, the spectra of the compressed gas at pressures up to 2,500 p.s.i. were examined in the region between  $1.80\mu$  and  $1.2\mu$ . This investigation also indicated no significant absorption which could be attributed to the continuum similar to that observed in the liquid. However, it is worthwhile noting that an indication of an absorption band was found at  $1.4\mu$  which could not be

explained in terms of any known impurity band; it is also found that the intensity of this band at a given pressure was not consistent for the different experiments. It is therefore concluded that the red continuum is absent in gaseous nitric oxide up to a density of approximately 150 Amagat units.

The nitric oxide molecule has a permanent dipole moment similar to that possessed by an oxygen molecule. It has been suggested that liquid nitric oxide is almost completely associated as  $(\text{NO})_2$  molecules (19) and a similar postulate has been made for liquid oxygen (14). Judging from the above suggestions, one might expect anomalous behaviour of absorption bands of nitric oxide in liquid as well as in high pressure gases since some anomalies have been found in liquid and high density gaseous oxygen spectra (7).

The above two continua in the infrared, red, and violet regions cannot be explained satisfactorily. Especially for the red continuum, it is hard to comprehend a mechanism of absorption in terms of the known behaviour of molecules. The absorption is definitely present only in the liquid and not in the gas and the extent of the absorption seems to be strongly dependent on the path length of the liquid. Although the information with regard to the window materials used in the absorption cells of previous investigators is not

available, the cutoff frequencies of the red band do not agree with the present results. It seems to indicate that the experimental conditions were also a determining factor for the extent of the absorption. Therefore, one may conclude that some impurity which is present only in liquid but not in gas, such as  $N_2O_3$ , could give rise to the absorption. It could also be suggested that the continuum is a series of unresolved bands which can be ascribed to transitions of  $(NO)_2$  molecules similar in nature to the "combination bands" of liquid oxygen, although the "combination bands" of oxygen have also been observed in compressed gases. However, one must postulate, then, the existence of electronic states of loosely bound  $(NO)_2$  molecules.

One could assume that the violet continuum may be ascribed to the dissociation of  $(NO)_2$  complexes; the dissociation energy of  $(NO)_2$  molecules in liquid NO could be computed from the frequency of the lower limit of the continuum. Taking the lower limit of the continuum to be at  $4140\text{\AA}$ , the dissociation energy was computed to be 3.0 electron volts.

In order to understand the nature of these continua fully, the following aspects must be emphasized in future investigations.

1. The study of the absorption in gaseous nitric oxide at higher pressures.

2. The study of the absorption in liquid NO using a very short absorption path length.
3. The entrance windows of the absorption cells may be changed to allow ultraviolet radiation into the cell to find the effect of this radiation on the red continuum.
4. The study of the absorption spectrum of  $\text{N}_2\text{O}_3$ ; which exist only below  $3.5^\circ\text{C}$ .
5. The study of the absorption spectrum of liquid NO introducing various degrees of impurity.

## APPENDIX

### A STUDY OF $7620\text{\AA}$ BAND OF OXYGEN IN LIQUID OXYGEN-ARGON MIXTURES

#### Experimental Procedure

The absorption band of the O-O transition of the "Red Atmospheric" Bands of oxygen was studied in liquid oxygen-argon mixtures. The absorption cell, which was used in the present investigation, has been described previously (4); the details of its construction are shown in Figure 14. The cell consisted of a glass cylinder 60 cm long and 7 cm in diameter with two glass crossarms, A, B. The vertical section, designed to contain the liquids, was sealed at the bottom with a circular flat aluminized pyrex plate M, which served as the reflecting mirror of the cell. The two crossarms, A, B, were fitted with brass lens housings, G, H; these lens housings held convex lenses for collimating and focusing the radiation. Vacuum seals between the lenses and the lens housings were obtained by means of O - ring seals. The two mirrors,  $M_1$ ,  $M_2$ , which were carried by a brass support, C, were suspended at the height of the crossarm. The support, C, and the adjusting screws, D, were brought out through the brass fitting, E, on the top of the cell and sealed by O - rings. The fitting, E, was attached to the top of the cell by plastic tape.

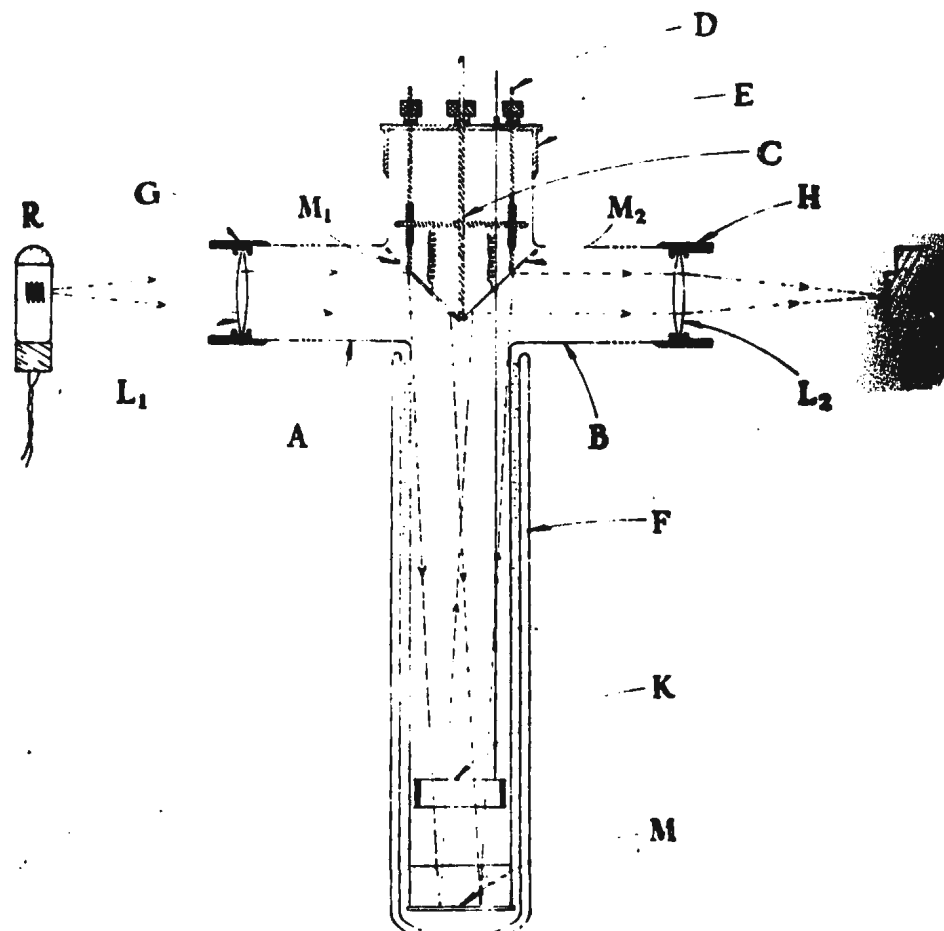


Figure 14. Low temperature liquid cell used in the investigation of liquid  $O_2$ -A mixtures.



The cell was equipped with a stirrer, K, which consisted of two thin brass rings; the stirrer was suspended from, E, by a glass rod sealed by an O - ring. The cell was placed in a vacuum flask, F, containing liquid air. The optical path through the cell is shown by the dotted lines in Figure 14. The radiation from a light source, R, was collimated by the lens, L<sub>1</sub>, and after reflection by the mirrors M, M<sub>1</sub>, and M<sub>2</sub>, was focused by means of the lens, L<sub>2</sub>, onto the slit of the spectrometer, S.

A Perkin-Elmer model 12-C recording infrared spectrometer with a dense flint glass prism was used in the present investigation. The spectral slit width used was 8 cm<sup>-1</sup>. The detector employed was an infrared sensitive photomultiplier tube, Dumont Type 6911; the optical arrangement for the photomultiplier tube is shown in Figure 15. The photomultiplier tube, A, which was housed in the brass light shield, B, was attached to the side exit window of the spectrometer, C, through an aluminum coupling, D. A light-proof seal of the photomultiplier was obtained by using black plastic tape on the outer wall of the photomultiplier tube and at the junction between B and D. The photomultiplier tube, A, was inserted in a socket contained in an enclosed circuit box, E. 1,400 volts DC from a John Fluke Power Supply model 400 BDA was applied between the anode and the cathode of the tube, A. The side exit window of the spectro-

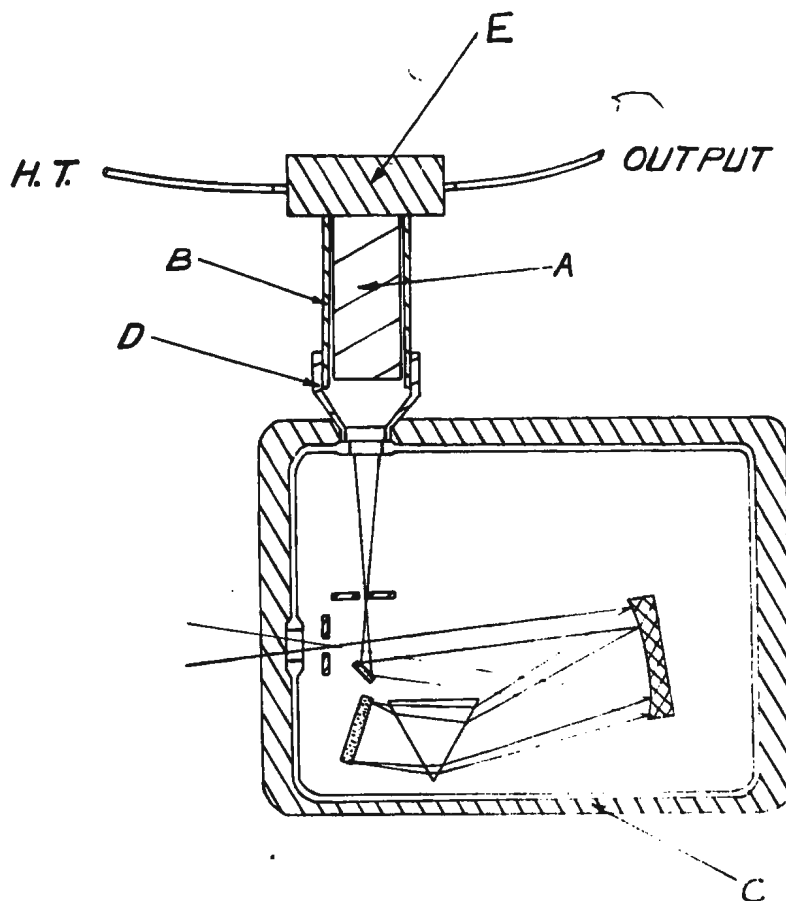


Figure 15. Photomultiplier attachment to the Perkin-Elmer 12C infra-red spectrometer.

meter, on which the photomultiplier was mounted, faces the exit slit of the spectrometer; no other alteration was made in the internal optics of the spectrometer.

After the cell was evacuated, oxygen gas from a commercial cylinder was condensed into the cell; prior to condensation the gas was passed through a trap at liquid air temperature which served as a drying trap. The mixtures were made by allowing argon gas to condense into the cell containing liquid oxygen. The concentrations of oxygen were calculated by taking the ratios of the volumes of pure oxygen to the volumes of the mixtures. In order to obtain accurate values for the volumes, cathetometer readings of liquid levels were taken from both sides of the cell and the average of the readings were used. After the liquids were mixed the stirrer was kept above the level of the liquid to avoid inaccuracy in the measurement of concentration.

A 750 watt projection lamp, operating on 60 cycle power supplied through a Sorenson Voltage Regulator, served as a light source. For wavelength calibration a neon discharge spectrum was used. The integrated absorption coefficients were found by the measurement of areas under the absorption contours; the absorption contours were produced by plotting absorption coefficients,  $\alpha$ , against the corresponding frequencies in  $\text{cm}^{-1}$ .

## Results

The study of the O-O "Red Atmospheric" band of oxygen in liquid oxygen-argon mixtures was carried out as a complimentary work to the investigation which has been conducted at the University of Toronto. The main purpose of this investigation was to find the effect of the dilution of liquid oxygen on the integrated absorption coefficient of the band. In this investigation it was hoped to make more accurate measurements of the absorption coefficient of the band since the recording spectrometer was used for the present study while previous investigations were carried out with a spectrograph for which very high accuracy in intensity measurement could not be claimed.

In Figure 16 is shown normalized contours for pure liquid oxygen and for 9.5% oxygen in liquid-argon mixtures. It can be seen that there is a marked change in the shape of the contour; the half width for the pure oxygen contour being  $129\text{ cm}^{-1}$  and that of the diluted oxygen being  $58\text{ cm}^{-1}$ .

There is also a shift in the peak of the band in the diluted oxygen from that in the pure liquid. The shift was observed to be approximately  $7\text{ cm}^{-1}$ . The values obtained with respect to the half width of the bands are in good agreement with the previous results of Cho. However, the change in the position of peaks is somewhat smaller than it

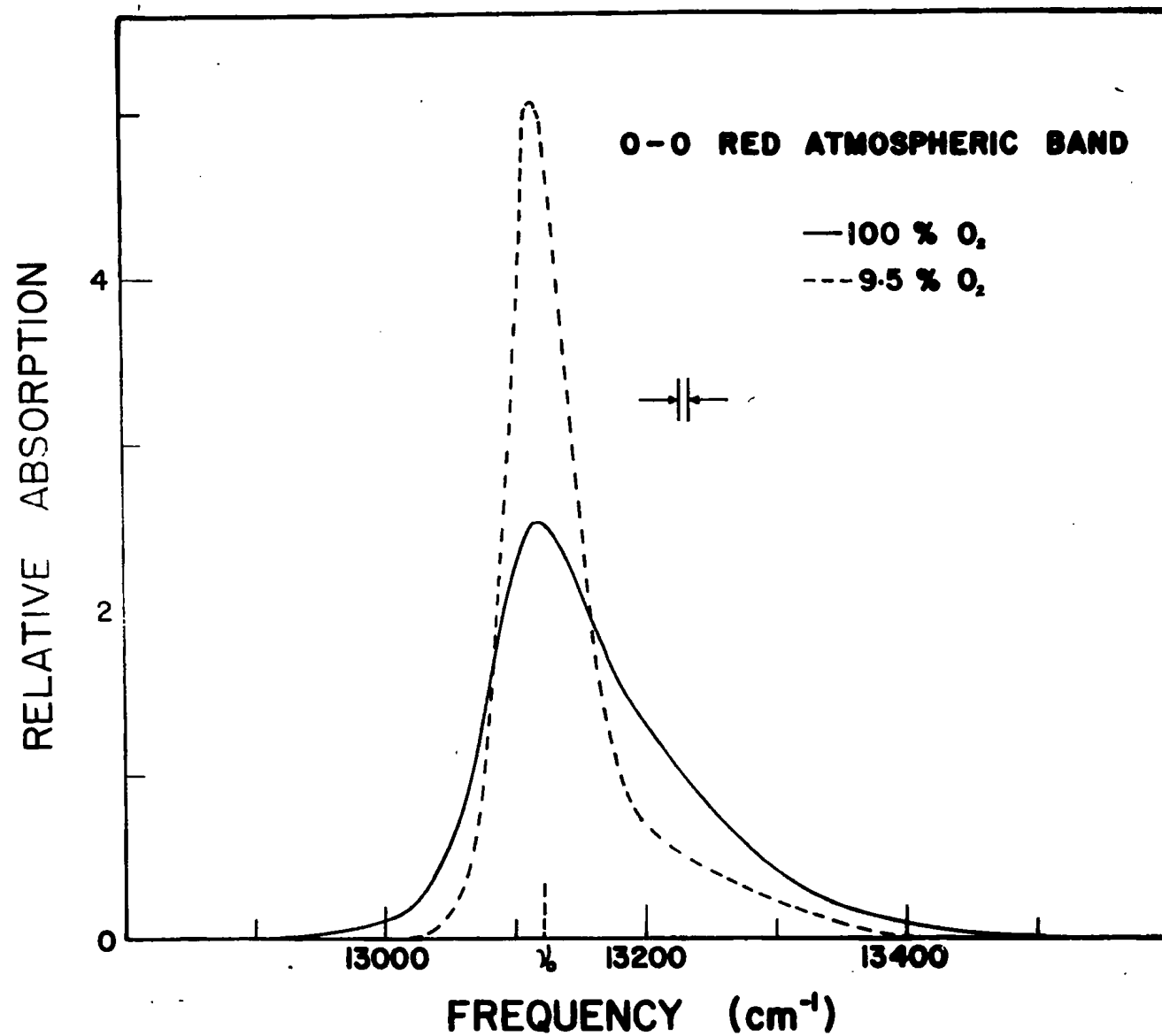


Figure 16. Normalized absorption contours of the 7620 Å band of oxygen.

is observed in the previous study ( $14 \text{ cm}^{-1}$ ) (4). This discrepancy could be explained as due to the wider spectral slit width used in this investigation ( $8 \text{ cm}^{-1}$  for the present and  $1.5 \text{ cm}^{-1}$  for Cho's).

In Table III is given a selection of experimental data for the band in liquid oxygen-argon mixtures at various concentrations of oxygen. In Figure 17,  $\int \alpha d\nu / \rho_{O_2}^2$  is plotted as a function of the partial density,  $\rho_{O_2}$ . The partial density of oxygen is computed by multiplying the concentration by the density, in Amagat Units, of the pure liquid oxygen at liquid air temperature,  $-188^\circ \text{ C}$ . In Figure 17, the previous data obtained by Cho (4) is also shown as a comparison. The graph shows that the integrated absorption coefficient is more or less proportional to the square of the partial density of oxygen at higher oxygen concentration; there are deviations from the square law at lower oxygen concentrations.

The integrated absorption coefficient can be expressed in general as a function of the partial density of oxygen by (4)

$$\int \alpha d\nu = A' \rho_{O_2} + B' \rho_{O_2}^2 + D' \rho_{O_2}^3$$

where  $A'$ ,  $B'$ , and  $D'$  are constants. Using the partial density of foreign gas,  $\rho_F$ , which can be approximated as:

$$\rho_F = (\rho_F)_{\text{PURE}} \left\{ 1 - \frac{\rho_{O_2}}{(\rho_{O_2})_{\text{PURE}}} \right\}$$

one can determine the relationship

Table III

INTENSITY DATA FOR THE 7620Å BAND OF  
OXYGEN IN LIQUID OXYGEN-ARGON MIXTURES

Concentration of O <sub>2</sub> (%)	Partial density of O <sub>2</sub> $\rho_{O_2}$ (Amagat Unit)	Integrated absorption coefficient (cm <sup>-1</sup> /cm)
100.	818.	23.7
100.	818.	25.8
100.	818.	21.6
89.1	729.	18.4
80.5	659.	15.1
70.7	578.	12.3
67.1	549.	12.0
43.4	355.	7.06
29.7	243.	3.31
9.50	77.8	0.75

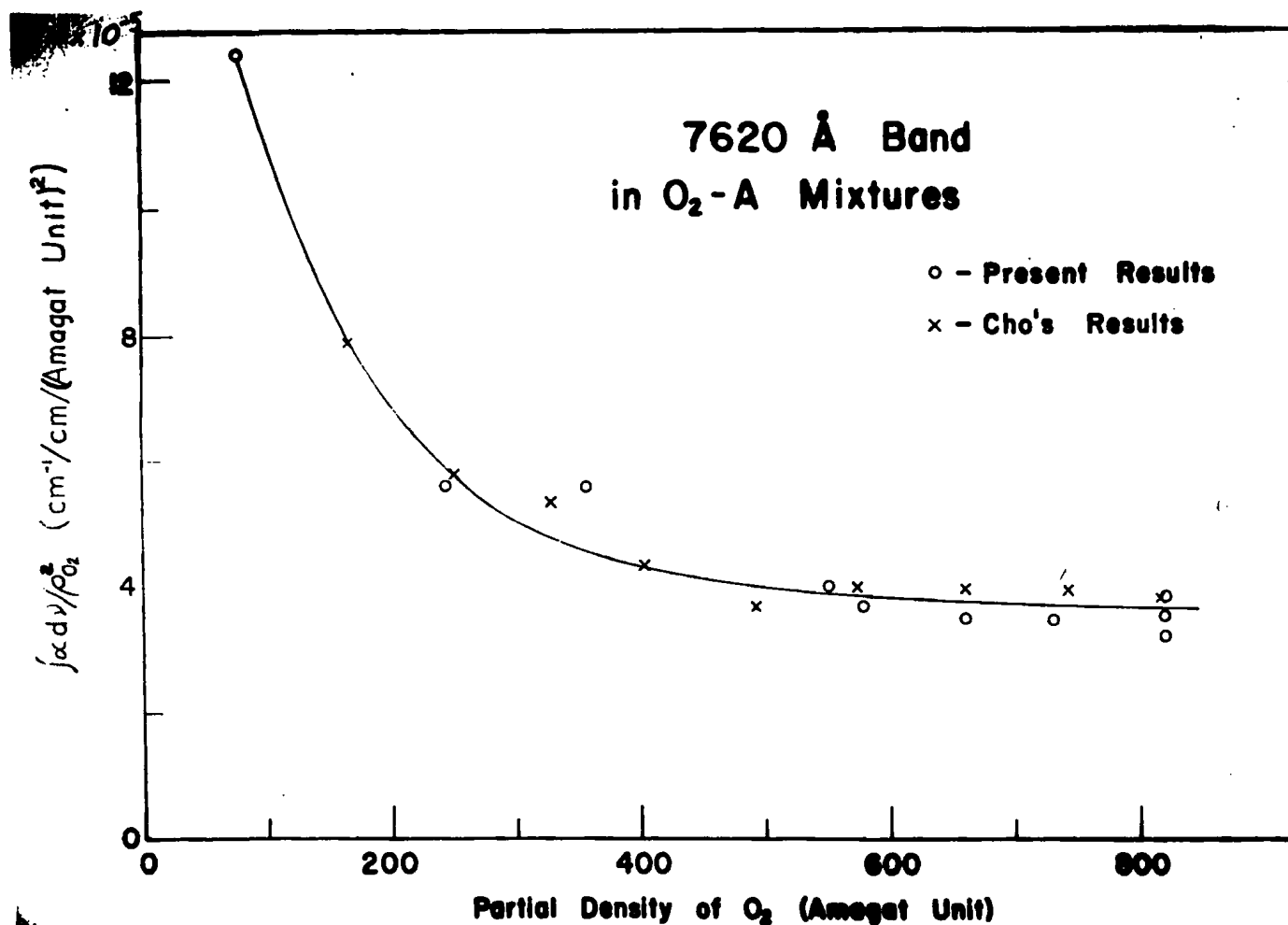


Figure 17. Dependence of the integrated absorption coefficient of the O-O red band on  $\rho_{O_2}$  in O<sub>2</sub>-A liquid mixtures.



$$\int \alpha dv = A \rho_{O_2} + B \rho_{O_2}^2 + C \rho_{O_2} \rho_F + D' \rho_{O_2}^3 + \dots$$

with  $A' = A + C (\rho_F)_{\text{pure}}$

$$B' = B - C \frac{(\rho_F)_{\text{pure}}}{(\rho_{O_2})_{\text{pure}}}$$

In these expressions  $(\rho_{O_2})_{\text{pure}}$  and  $(\rho_F)_{\text{pure}}$  represent the densities of the pure liquids and A and B are constants.

Following the same procedure as is given by Cho (4) the coefficients A', B', and D' are obtained:

$$A' = .90 \times 10^{-2}$$

$$B' = 2.3 \times 10^{-5}$$

$$D' = .9 \times 10^{-8}$$

These values are in very good agreement with the previous results.

## SUMMARY

The second overtone rotation-vibration band of nitric oxide has been studied in pure liquid and in compressed pure gas. Although the band was not observed in liquid nitric oxide, due to the presence of a strong absorption continuum, the band was observed in the compressed gaseous nitric oxide at pressures ranging from 1 - 150 atmospheres; it was found that the shape of the band did not change within this pressure range. The appearance of the band was very similar to the Bjerrum double band. The rotational constant  $B$  was calculated; the observed value of the constant  $B$  was found to be in very good agreement with the known value. The integrated absorption coefficient of the band varied nearly linearly with the density of the gas, however, a small quadratic term, which is supposed to be responsible for the pressure induced absorption, was also observed.

The absorption of nitric oxide in liquid nitric oxide was also studied and two absorption continua were observed; one starting in the red region of the spectrum and extending toward the infrared region and the other starting in the violet region of the spectrum and extending toward the ultraviolet region. Assuming that the violet continuum was due to  $(\text{NO})_2$  complexes the dissociation energy of these complexes was calculated from the cutoff frequency of the violet continuum; this dissociation energy was found to be

3.0 ev. There was a strong suspicion that the red continuum arises from  $N_2O_3$  impurity in the liquid nitric oxide, however, this assumption should be checked in future investigations.

In the course of this research a short study of the  $7620\text{\AA}$  band of  $O_2$  was made in liquid  $O_2$ -A mixtures as a complimentary work to the investigation which had been carried out at the University of Toronto. The results obtained in this investigation were in very good agreement with the previous results.

## BIBLIOGRAPHY

- (1) Barton, H. A. and Mulliken, R. S., Phys. Rev. 30, 150 (1927)
- (2) Bernstein, H. J. and Herzberg, G., J. Chem. Phys. 15, 77 (1947)
- (3) Burrus, C. A. and Gordy, W., Phys. Rev. 93, 729 (1954)
- (4) Cho, C. W., Ph.D. Thesis, University of Toronto (1958)
- (5) Clouter, M. J., M. Sc. Thesis, Memorial University of Newfoundland (1962)
- (6) Dennison, D. M., Rev. Mod. Phys. 3, 315 (1931)
- (7) Ellis, J. W. and Kneser, O., Zeits. f. Phys. 86, 583 (1933)
- (8) Gero, L., Schmid, R. and Von Szily, K. F., Physica 11, 144 (1944)
- (9) Gillette, R. H. and Eyster, E. H., Phys. Rev. 56, 1112 (1939)
- (10) Golding, B. H. and Saye, B. H., Ind. Eng. Chem. 43, 160 (1951)
- (11) Gush, H. P., Private Communication
- (12) Herzberg, G., Spectra of Diatomic Molecules, 2nd Ed. D. Van Nostrand
- (13) Johnson, H. H. & Glaugae, W. F., J. Amer. Chem., Soc. 51, 3194 (1929)
- (14) Lewis, G. N., J. Amer. Chem. Soc. 46, 2027 (1924)
- (15) Mulliken, R. S., Rev. Mod. Phys. 2, 109, (1930)
- (16) Nichols, N. L., Hause, C. D. and Noble, R. H., J. Chem. Phys. 23, 57 (1955)
- (17) Nielsen, A. H. and Gordy, W., Phys. Rev. 56, 781 (1939)
- (18) Penner, S. S. & Weber, D., J. Chem. Phys. 21, 649 (1953)
- (19) Rice, O.K., J. Chem. Phys. 4, 367 (1936)

- (20) Schmid, R., Z. Physik 49, 428 (1928)  
       "      "      "      " 64, 84 (1930)
- (21) Schmid, R., Z. Physik 64, 229 (1930)
- (22) Shaw, J. H., J. Chem. Phys. 24, 399 (1956)
- (23) Smithsonian Physical Tables 120, 49 9th Ed.
- (24) Snow, C. P., Rawlins, F. I. G., and Rideal, E. K.  
       Proc. Roy. Soc. A124, 460(1929)  
       "      "      "      " A126, 356(1930)
- (25) Stevenson, C. M., Private Communication
- (26) Tanaka, Y., Sci. Pap. Inst. Phys. Chem. Res. (Tokyo) 39,  
       456 (1942)
- (27) Vodar, M. B., Comptes rendus 204, 1467 (1937)
- (28) Warburg, E., and Leithauser, G., Ber. deut. chem. Ges.  
       1, 145 (1908)

## ACKNOWLEDGMENTS

The research described in this thesis was supervised by Professor C. W. Cho to whom the author is greatly indebted for guidance during the course of the experimental work and in the preparation of the thesis.

The writer wishes to express his gratitude to the workshop staff, especially Mr. T. W. Gordon, for their skilful workmanship and advice and also to Mr. C. M. Stevenson for his assistance during the experimental work and for producing the diagrams used in the thesis.

The author is greatly appreciative of the loan of the low temperature liquid cell by the University of Toronto.

The assistance of Mrs. C. W. Cho in typing the thesis is gratefully acknowledged.

Thanks are also gratefully rendered to Professor J. L. Hunt and to Mr. M. J. Clouter for their assistance and advice.









